Structure of buffalo lactoferrin at 2.5 Å resolution using crystals grown at 303 K shows different orientations of the N and C lobes

**Subramanian Karthikeyan,
Murugan Paramasivam, Savita
Yadav, Alagiri Srinivasan and
Tej P. Singh***

Department of Biophysics, All India Institute of
Medical Sciences, New Delhi 110 029, India

Correspondence e-mail: tps@medinst.ernet.in

The structure of buffalo lactoferrin has been determined at 303 K. The crystals belong to orthorhombic space group $P2_12_12_1$, with unit-cell parameters $a = 77.5$, $b = 91.0$, $c = 131.5$ Å and $Z = 4$. The structure has been refined to an R factor of 0.187. The overall structure of the protein is similar to its structure determined at 277 K in a different crystal form. However, the lobe orientations in the two structures differ by $9.0°$, suggesting significant inter-lobe flexibility in this family of proteins. The inter-lobe interactions are predominantly hydrophobic and could act as a cushion for a change in orientation under the influence of external conditions. On the other hand, the domain arrangements are found to be similar in 277 and 303 K crystal structures, with orientations differing by 1.5 and $1.0°$ in the N and C lobes, respectively. The results of these investigations suggest that the increase in temperature helps in the production of better quality crystals.

1. Introduction

Lactoferrin is a member of the transferrin family of proteins. It is a monomeric glycoprotein with a molecular weight of approximately 80 kDa. It consists of a single polypeptide chain folded into two homologous N and C lobes. Both the N and C lobes contain about 345 amino acids and are made up of two domains: N1 and N2 in the N lobe and C1 and C2 in the C lobe. These proteins fulfil a key role in controlling the levels of free iron in the body fluids of animals. These bilobate molecules have two binding sites, one per lobe, each housing Fe^{3+} and synergistic CO_3^{2-} ions (Karthikeyan, Sharma *et al.*, 1999). Other functions of lactoferrin include antibacterial activity (Arnold *et al.*, 1977), role as a growth factor (Hashizume *et al.*, 1983), modulation of the immune and inflammatory responses (Birgens *et al.*, 1983) and specific DNA binding (He & Furmanski, 1995). Most of these functions differ considerably according to species and are attributable to the specific elements of three-dimensional structure, highlighting the importance of structural comparisons. Three-dimensional structures of human lactoferrin (Anderson *et al.*, 1989), bovine lactoferrin (Moore *et al.*, 1997), mare lactoferrin (Sharma, Paramasivam *et al.*, 1999), rabbit serum transferrin (Bailey *et al.*, 1988), hen ovotransferrin (Kurokawa *et al.*, 1995) and duck ovotransferrin (Rawas *et al.*, 1996) in their iron-bound forms have characterized their iron-binding sites and the protein structure in the iron-bound state, in which both the N and C lobes adopt closed conformations. The structures of human lactoferrin (Anderson *et al.*, 1990), duck ovotransferrin (Rawas *et al.*, 1997) and mare lactoferrin (Sharma, Raja-shankar *et al.*, 1999) in their iron-free (apo) forms have revealed different domain arrangements, *i.e.* in duck

ovotransferrin both lobes are in the open conformation, in human apolactoferrin the N lobe is in the open conformation and the C lobe adopts a closed conformation, while in mare apolactoferrin both lobes are in the closed conformation. These results indicate that iron binding can take place in the lobes in both the open and closed forms, thus giving rise to further questions regarding the mechanism of iron binding and release and its relationship to conformational changes in the protein. An open question is whether or not the open conformations of the lobes are necessary for iron binding. If not, why do some proteins of the family adopt open conformations as opposed to others? Are there other functions related to the different conformational forms of the apo proteins? Can those functions be understood in terms of inter-domain interactions? Are inter-domain interactions affected by the external environment? What happens to inter-lobe associations under different conditions? Can the inter-molecular interactions be influenced by changing the temperatures of the crystallization set-ups? Are inter-domain and inter-lobe interactions conserved in these proteins? In order to answer the above questions, it was necessary to analyze the crystal structures of lactoferrin from a number of species and under different conditions. We have previously reported the three-dimensional structure of buffalo lactoferrin (blf1) at 3.3 Å resolution using crystals grown at 277 K (Karthikeyan, Yadav *et al.*, 1999). So far, all the proteins of the transferrin family have been crystallized at 277 K and the quality of crystals has varied, presumably according to the glycan content. The crystals of human lactoferrin were the best (diffracting to 2.2 Å resolution) with the least number of glycan chains (two), while those of bovine and buffalo lactoferrin were relatively poor (diffracting to 2.8 and 2.5 Å resolutions, respectively) with the largest number of glycan chains (4–5). In any case, most of these structures reported low levels of crystal packing interactions. In order to improve the quality of crystals and to evaluate the roles of external conditions on the domain arrangements, lobe orientations and the overall structure of the protein, we have crystallized buffalo lactoferrin (blf2) at 303 K.

Here, we present the three-dimensional structure of buffalo lactoferrin determined by the X-ray diffraction method at 2.5 Å resolution. Crystals of a member of the transferrin family were grown at 303 K for the first time and the intensity data were also collected at 303 K. This study provides new insights into the role of inter-domain and inter-lobe interactions and their mutual orientations and has revealed aspects of the structure sensitive to environmental fluctuations.

2. Experimental

2.1. Purification

Buffalo milk was obtained from the National Dairy Research Institute, Karnal (India). Purification was carried out using a locally modified procedure (Raman *et al.*, 1992). Diluted colostrum/milk was defatted by skimming. Skimmed milk was diluted twice with 0.05 M Tris–HCl pH 8.0. CM-

Sephadex C-50 was added to it (7 g l^{-1}) and stirred slowly using a mechanical stirrer for 1 h. The gel was allowed to settle and the milk was then decanted. The gel was washed with an excess of 0.05 M Tris–HCl pH 8.0, packed in a column (25 × 2.5 cm) and washed with the same buffer containing 0.1 M NaCl, which facilitated the removal of impurities. The lactoferrin was then eluted with same buffer containing 0.25 M NaCl. The protein solution was dialysed against an excess of triple-distilled water. The protein was again passed through a CM-Sephadex C-50 column (10 × 2.5 cm) pre-equilibrated with 0.05 M Tris–HCl pH 8.0 and eluted with a linear gradient of 0.05–0.3 M NaCl in the same buffer. The protein was concentrated using an Amicon ultrafiltration cell. The concentrated protein was passed through a Sephadex G-100 column (100 × 2 cm) using 0.05 M Tris–HCl buffer pH 8.0. The purity of the lactoferrin was confirmed by sodium dodecyl sulfate polyacrylamide gel electrophoresis (SDS–PAGE; Laemmli, 1970).

2.2. Preparation of iron-saturated lactoferrin

The iron-saturated lactoferrin was prepared following the procedure of Mazurier & Spik (1980). The purified lactoferrin was dissolved in 1 ml of 0.1 M sodium bicarbonate buffered with sodium citrate at pH 8.0 to obtain a concentration of 1 mM. To this solution, 1.2 ml of ferric chloride reagent (2 mM FeCl$_3$.6H$_2$O in 0.1 M sodium bicarbonate buffered with sodium citrate at pH 8.0) was added and equilibrated for 24 h at 298 K. The excess of ferric chloride reagent was removed by passing the preparation through a Sephadex G-50 column (50 × 2.0 cm) and eluting with distilled water. The iron content was estimated by a modified procedure of Wootton (1964) using tripyridyl reagent and was found to be 92%.

2.3. Crystallization

Iron-saturated lactoferrin samples were used for crystallization. Crystals suitable for X-ray diffraction were obtained by the microdialysis method with protein concentrations in the range 50–70 mg ml^{-1} in 0.025 M Tris–HCl at pH 8.0. This solution was dialyzed against the same buffer containing 19%(v/v) ethanol at pH 8.0. All crystallization experiments were carried out at 303 K. Deep-red crystals grew in two weeks to dimensions of 0.5 × 0.3 × 0.2 mm. These crystals tended to redissolve in their mother liquors, very often transformed into an oil at room temperature and sometimes lost their orderliness soon after their removal from the dialysis tubes. The crystals were stable in a harvesting buffer containing 20% MPD. Therefore, the crystals were transferred to a buffer containing 25 mM Tris–HCl pH 8.0, 19%(v/v) ethanol and 20% MPD for data collection. Using this buffer, the crystals were stable for about 48 h in the X-ray beam.

2.4. Data collection

For data collection, crystals were mounted in glass capillaries. X-ray intensities were measured at 303 K (the ambient room temperature was kept at 303 K) using a MAR Research imaging-plate scanner with a diameter of 300 mm. It might be

Table 1
Crystallographic data, data-collection and refinement-model statistics.

Space group	$P2_12_12_1$
Number of molecules in the cell	4
Unit-cell dimensions (a, b, c) (Å)	77.5, 91.0, 131.5
Resolution range (Å)	15.0–2.5
Total number of reflections	29307
Overall completeness (%)	90.0
R_{merge} for all data (%)	6.9
Completeness in outer shell (2.6–2.5 Å) (%)	76.1
R_{merge} for the outer shell (2.6–2.5 Å) (%)	19.4
Model	
Number of protein atoms	5314
Number of ferric ions	2
Number of carbonate ions	8
Number of solvent atoms	91
Average B factors (Å^2)	
Main-chain atoms	53.3
Side-chain atoms	56.6
Ferric ions	38.4
Overall	55.0
Stereochemistry	
R.m.s bond length	0.006
R.m.s bond angle (°)	1.3
R.m.s dihedral angle (°)	26.0
Refinement	
Resolution limits (Å)	15.0–2.5
R factor	0.187
R_{free} (5% data)	0.265

mentioned here that the data on the crystals grown at 277 K were collected at 277 K (Karthikeyan, Yadav *et al.*, 1999). The crystal-to-detector distance was kept at 200 mm. Monochromatic Cu $K\alpha$ radiation was produced by a graphite-crystal monochromator mounted on a Rigaku RU-200 rotating-anode generator operating at 40 kV and 100 mA with a focal point of 3×0.3 mm. Two crystals were used for the complete intensity data collection. The crystals diffracted to 2.5 Å resolution.

2.5. Data processing

The *HKL* package (Otwinowski & Minor, 1997) and *MARSCALE* (Kabsch, 1986) were used for the determination of unit-cell parameters, data processing, scaling and merging. The crystals belong to orthorhombic space group $P2_12_12_1$, with one molecule in the asymmetric unit. The unit-cell parameters are $a = 77.5$, $b = 91.0$, $c = 131.5$ Å. The crystals have a V_m value (Matthews, 1968) of 2.90 Å^3 Da^{-1} for one molecule in the asymmetric unit. This corresponds to a solvent content of 57.6%. X-ray intensity data were collected to 2.5 Å resolution. The data set is 90% complete, with 29307 unique reflections in the resolution range 15–2.5 Å. R_{merge} was 0.069. The details of the crystallographic data collection and processing statistics are given in Table 1.

2.6. Structure solution

The structure was determined by the molecular-replacement method employing the *AMoRe* program (Navaza, 1994) incorporated in the *CCP*4 package (Collaborative Computational Project, Number 4, 1994), using the monoclinic 277 K structure of diferric buffalo lactoferrin as a model. The rotation function was calculated using diffraction data in the resolution range 10–5 Å with a sphere radius of 25 Å. The first

peak appeared as a distinct solution. The top peak of the rotation function yielded an even more distinct top solution peak in the translation function, with a correlation coefficient of 38.7% and an R factor of 51.6%. After rigid-body refinement, the correlation coefficient and R factor were 40.0 and 48.9%, respectively.

2.7. Structure refinement

The model obtained from molecular replacement was refined using the program *X-PLOR* (Brünger *et al.*, 1987; Brünger, 1992*a*). Prior to refinement, all temperature factors were reset to 30 Å^2. A randomly chosen 5% of the reflections in the data set were used for R_{free} calculations (Brünger, 1992*b*). Rigid-body refinement, taking the N lobe (residues 1–344) and the C lobe (residues 34–689) as two separate rigid bodies, lowered the R factor to 0.390 ($R_{free} = 0.441$). Further cycles of refinement and model building using 'positional' and 'prepstage' in *X-PLOR* protocol lowered the R factor to 0.321 ($R_{free} = 0.401$). The electron densities for the two Fe^{3+} ions, two CO_3^{2-} ions and side chains involved in metal binding were now well defined. Subsequent refinement cycles of simulated annealing (Brünger *et al.*, 1990) and restrained least-squares refinement followed by manual model building (Jones *et al.*, 1991) were carried out to improve the model. The temperature-factor refinement for individual atoms lowered the R
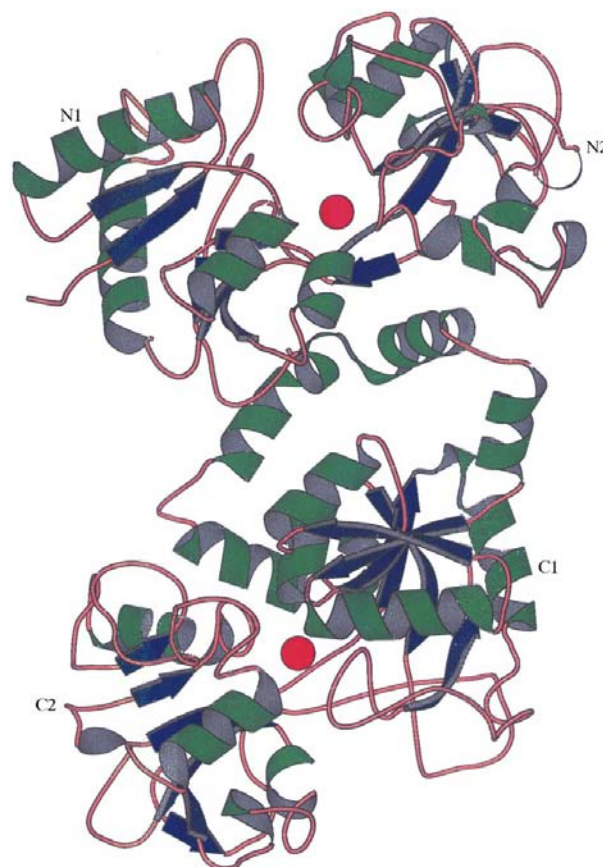

Figure 1
Three-dimensional folding of buffalo lactoferrin molecule. The figure was drawn using *MOLSCRIPT* (Kraulis, 1991).

factor to 0.221. Water molecules were added where the difference density had values of more than 3σ above the mean and the $2F_o - F_c$ map showed density at greater than the 1σ level. The final R factor was 0.187 for all data to 2.5 Å resolution. The final refinement statistics are given in Table 1.

3. Results and discussion

3.1. Quality of the final model

The final model consists of 5314 protein atoms from 689 amino-acid residues, two Fe^{3+} ions, two CO_3^{2-} ions and 91 water molecules. The protein structure has geometry close to ideal, with r.m.s. deviations of 0.006 Å and 1.3° from standard values for bond lengths and angles, respectively. The final crystallographic R factor for all 29 307 reflections was 18.7% and R_{free} was 26.5% (Table 1). The overall mean B factor for the structure is 55.0 Å^2, which appears to be high but is still considerably lower than the 71.4 Å^2 observed in bovine lactoferrin (clf). As seen from the final $2F_o - F_c$ map, the structure is well defined without any break in the backbone. A Ramachandran plot of the main-chain torsion angles (φ, ψ) (Ramachandran & Sasisekaran, 1968) shows that 84.3% of the residues are in the most-favoured regions as defined in the program *PROCHECK* (Laskowski *et al.*, 1993). Only two residues are in normally disallowed regions, but these (Leu299 and Leu640) are the central residues in two γ-turns (Matthews, 1972) and have (φ, ψ) values typical of such conformations, around (70, −60°). These two γ-turns are conserved in the N and C lobes of lactoferrin and transferrin structures (Bailey *et al.*, 1988; Haridas *et al.*, 1995; Kurokawa *et al.*, 1995; Moore *et al.*, 1997; Sharma, Paramasivam *et al.*, 1999).

3.2. Overall molecular structure

Buffalo lactoferrin consists of 689 amino-acid residues with a molecular weight of 75 707 Da (Karthikeyan, Sharma *et al.*,
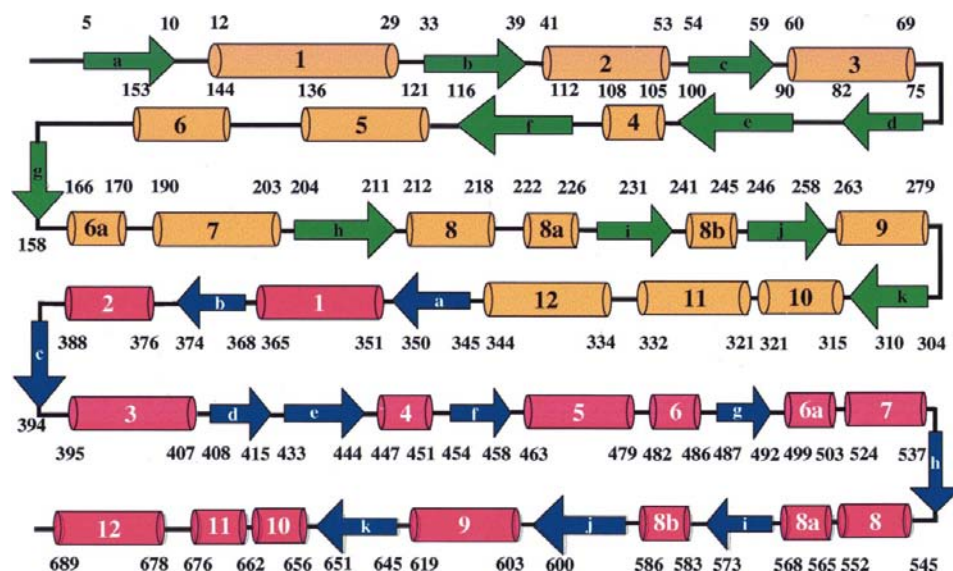
Table 2
Superposition of C lobe on N lobe.

Structure	R.m.s deviation (Å)			Rotation angle† (°)
	N1–C1	N2–C2	N–C	
blf1	1.37	0.94	1.34	5.9
blf2	1.19	0.89	1.31	6.1
clf	1.27	0.88	1.29	6.5
mlf	1.35	0.81	1.11	1.1
hlf	1.07	0.87	1.18	6.2
otf	0.97	1.01	1.24	5.1

† Rotation needed to best fit the C2 domain onto the N2 domain after the N1 and C1 domains have been superimposed.

1999). The protein is folded into two lobes (the N and C lobes, representing the N-terminal and the C-terminal halves of the polypeptide), each of which is divided into two domains (N1 and N2, and C1 and C2; Fig. 1). In each lobe, the iron-binding site lies between the two domains. The N and C lobes are linked by a three-turn connecting α-helix (residues 334–344). The elements of secondary structure are indicated in Fig. 2.

The high level of sequence identity (41%) between the two halves of the molecule is reflected in a very similar folding of the polypeptide chain in the two lobes. The two lobes are related by an approximate twofold screw axis, the C lobe being superimposable on the N lobe by a rotation of 177.3° and a translation of 24.7 Å. When the two lobes are superimposed after matching N1 on C1, the additional rotation angle required for the best fitting of N2 with C2 in blf2 is 6.1°. This finding shows that the relative orientations of the domains in the N and C lobes are not identical. As seen from Table 2, similar values are found in blf1, bovine lactoferrin (clf), human lactoferrin (hlf) and duck ovotransferrin (otf), where the domain orientations in the N and C lobes can be considered significantly different, whereas in mare lactoferrin (mlf), the orientations of the N1 and N2 domains are almost identical to the orientations of the C1 and C2 domains (Table 2).

Although the overall folding of the protein at 303 K is similar to that observed at 277 K, some individual residues are displaced significantly. When the structure of buffalo lactoferrin at 277 K (determined in a different crystal form) was superimposed on the structure at 303 K, it showed an r.m.s. deviation of 1.37 Å for the C$^\alpha$ atoms and 1.39 Å for all the main-chain atoms. When the N lobes of the two structures were superimposed, an additional rotation of the C lobe of 9.0° was required to bring the C lobe into correspondence (Fig. 3). This showed that the lobe orientations have changed substantially on raising the temperature of the system from 277 to 303 K. The corresponding values

Figure 2
Schematic representation of secondary-structure elements.

Table 3
Superposition of blf2 on other iron-saturated lactoferrins and transferrins.

Structure†	R.m.s. deviations for C^α atoms‡ (Å)	Angle of rotation for C lobe§ (°)	PDB code
blf1	1.4	9.0	1biy
clf	1.2	7.0	1blf
mlf	1.9	15.4	1b1x
hlf	1.7	14.8	1lfg
otf	2.4	24.0	1dot

† All the structures are with Fe^{3+}. ‡ When all C^α atoms have been used in the superposition. § After the structures have been superimposed based on the C^α coordinates of the N-lobes.

for superposition of blf2 onto other lactoferrins and duck ovotransferrin are listed in Table 3.

The superposition of individual lobes of blf1 and blf2 showed an r.m.s. deviations of 0.60 Å for the N lobes and 0.67 Å for the C lobes. In order to achieve complete superposition of lobes, an additional rotation of individual domains was necessary. When the N1 domains were superimposed, an additional rotation of 1.5° of the N2 domain was required. Similarly, in the case of the C lobe, an additional rotation of 1.0° of the C2 domain was necessary to superimpose the C lobes of the two structures. A further superposition of individual domains indicated the deviations for C^α atoms to be 0.60 Å for N1 domains, 0.54 Å for C1 domains, 0.67 Å for N2 domains and 0.56 Å for C2 domains. These data clearly indicate that the domain arrangements are only slightly affected by raising the temperature to 303 K.

3.3. Comparison with other lactoferrins

When the two structures of buffalo lactoferrins, blf1 and blf2, were compared with other lactoferrins and duck ovotransferrin, a clear trend in the relative shifts of their structures was observed. The r.m.s. shifts among lactoferrins (C^α shifts $\leq$ 2.0 Å) were found to be smaller than those

between lactoferrins and transferrins (C^α shifts $\geq$ 2.0 Å). On comparing C^α traces of blf1 with clf, mlf, hlf and otf, the r.m.s. shifts were found to be 0.79, 1.28, 1.44 and 2.35 Å, respectively. The corresponding values for blf2 were 1.18, 1.86, 1.72 and 2.39 Å, respectively. These systematic differences clearly indicated the effect of temperature. On extending this analysis to individual lobes, the overall r.m.s. shifts for C^α atoms were less than 1 Å. The r.m.s shifts were even smaller when individual domains were compared ($\leq$0.5 Å). These observations indicated the largest effect on the relative orientations of the lobes.

Similarly, the superpositions of blf1 and blf2 on the structures of other lactoferrins and ovotransferrins for the whole molecule and individual lobes have also been analyzed with respect to rotation of domains and lobes. On superimposing the N lobes of blf1 and blf2 on the N lobes of clf, mlf, hlf and otf, significant rotations of the C lobes are needed to bring the two lobes into an appropriate correspondence. The values of rotation angles for blf1 with respect to clf, mlf, hlf and otf were found to be 3.3, 6.9, 8.0 and 21.2°, respectively. The corresponding values for blf2 are 7.0, 15.4, 14.8 and 24.1°, respectively. The values for blf2 are almost twice as large as those for blf1 in the case of lactoferrins and significantly larger in the case of ovotransferrin. Once again, this finding demonstrates the flexibility of inter-lobe arrangements. In the case of superposition of individual lobes of blf1 and blf2 on other lactoferrins and ovotransferrin, no systematic differences have been observed, except that the domains in the N lobes are slightly more flexible than those in the C lobes. Furthermore, there exists no trend between the values observed for blf1 and blf2, thus suggesting that the domain arrangements are not perturbed by environmental variations.

3.4. Inter-domain interactions

The iron binding and release in the proteins of the transferrin family were considered to be associated with large domain movements, as these proteins changed between an open form characteristic of the iron-free protein to a closed form characteristic of the iron-bound protein (Anderson *et al.*, 1990). Therefore, it was believed that the interactions between the domains played a major part in retarding or enhancing the ease of iron binding and release.

The binding cleft of each lobe is highly polar and is formed by the inner surfaces of two domains. The wall provided by domain I comprises the N-termini of helices 1, 2 and 3, together with a section of polypeptide (293–302 in the N lobe, 632–640 in the C lobe) which is made up of a series of turns, including the conserved γ-turn 297–299. The wall provided by domain II comprises the N-termini of helices 5 and 7, one side of helix 8 and a loop (182–185 in the N lobe, 513–516 in the C lobe) at the mouth of the cleft.
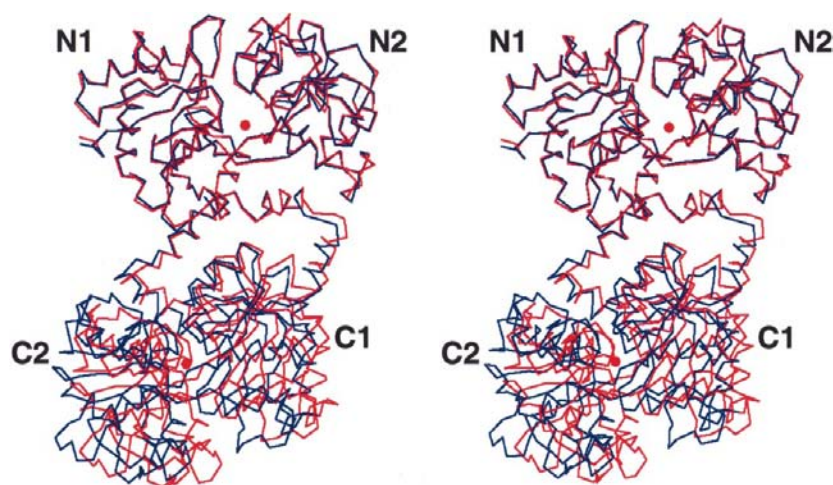

Figure 3
Superimposition of the C^α traces of blf1 (red) and blf2 (blue) on the basis of the N lobe only.

As observed in other lactoferrins, there are several direct hydrogen-bonded interactions across the binding cleft between the two domains of each lobe. In both lobes, there are a few hydrogen bonds which are associated with the ligands of iron sites, involving Asp60 and Ser122 in the N lobe and Asp395 and Thr464 in the C lobe. These hydrogen bonds are present in all proteins of the transferrin family (Kurokawa *et al.*, 1995). A typical interaction at the mouth of the binding cleft in the N lobe of other lactoferrins involving Ser185 is absent in buffalo lactoferrin, as Ser185 becomes Pro185. In place of this interaction, buffalo lactoferrin has two new interactions formed by Ala40···Ser184 and Asn126···Tyr324, which are absent in other lactoferrins. In bovine lactoferrin, residue 126 is Ile. In the C lobe, in addition to two hydrogen bonds through the iron site, there are seven other hydrogen bonds which directly link the protein atoms of two domains.

Other contributions to inter-domain interactions, and thus to the stability of the closed form, come from van der Waals contacts and possibly from interactions *via* water molecules at the interface. However, the sequence changes which occur in the domain interface of buffalo lactoferrin seem to suggest a reduction in bulk of the side chains when compared with human lactoferrin (N lobe: Pro42→Ala, Pro63→Met, Thr122→Ser, Phe183→Cys; C lobe Glu352→Pro). This could mean that the domains in buffalo lactoferrin might be closer together in order to attain a better fit.

3.5. Interactions between the lobes

The large differences in relative orientations of N and C lobes in transferrins were attributed to differences in the conformations of the inter-lobe connecting region (residues 334–345; Kurokawa *et al.*, 1995). This is unlikely to be the case in lactoferrins, because in all of them a regular α-helix of the same length (11 residues) connects the two lobes. The studies on buffalo lactoferrin at two different temperatures have indicated that the association of N and C lobes is flexible. The inter-lobe interactions are overwhelmingly hydrophobic. The sliding of lobes can occur owing to external forces including

crystal packing. The sequence mutations at the inter-lobe interface can also cause variations in the orientations of two lobes.

The contact region between two lobes comprises helices α10 and α11 from the N lobe, together with a preceding loop 209–314, and α2 and α12 from the C lobe. The only direct interaction in the structure at 277 K is a salt bridge Asp315···Lys386, whereas in the structure at 303 K, in addition to the above interaction, two more hydrogen bonds have been observed: Lys313···Asp379 and Lys329···Lys386. The earlier experiments on the proteolytic production of two molecular halves using proteinase K have shown that the N and C lobes tended to aggregate in the gel-filtration column. They could be kept separate with the help of detergents and organic solvents (Singh *et al.*, 1998). The residues which are main contributors on the N lobe are Thr90, Leu308, Ile310, Pro311, Lys313, Asp315, Leu318, Tyr319 and Leu325, and on the C lobe, Leu385, Lys386, Pro679, Phe686 and Arg689. Although the contacts are not very close, these side chains provide a hydrophobic cushion between the two lobes and solvent is excluded from this region. The difference in the relative orientations of the two lobes in the structures of buffalo lactoferrin at 277 and 303 K can be traced to a slight repacking of this hydrophobic surface. The same logic can be extended to the observed differences in the relative orientations of the lobes in other lactoferrins and transferrins.

3.6. Metal- and anion-binding sites

The metal- and anion-binding sites are similar in both lobes. The two iron sites, situated one in each lobe at the end of each interdomain cleft, are 44.2 Å apart. The Fe atoms are deeply buried, the minimum distance from the molecular exterior in each lobe being approximately 10 Å. Their environment is highly polar, with numerous polar side chains in their vicinity.

The two iron sites have an almost identical (immediate) coordination environment. The geometry of iron is distorted octahedral in both sites, with four protein ligands and two non-protein ligands occupying the six octahedral positions around the Fe atom. Four protein ligands are provided by one carboxylate O atom, two phenolate O atoms and one imidazole ring N atom. In the N lobe, the iron ligands are Asp60, Tyr92, Tyr192, His253 and CO_3^{2-} ion, and in the C lobe, Asp395, Tyr433, Tyr526, His595 and CO_3^{2-} ion (Fig. 4). All four ligating residues are widely spaced along the polypeptide chain and belong to distinct parts of the protein structure. The two O atoms from the carbonate ion complete the octahedral geometry by occupying the remaining two *cis* positions. Each of the two coordinated carbonate O atoms accepts a hydrogen bond through its remaining lone pair (O1 from a peptide NH; O2 forms a bifurcated hydrogen bond from the NH1 and NE H atoms of the Arg121 residue) and
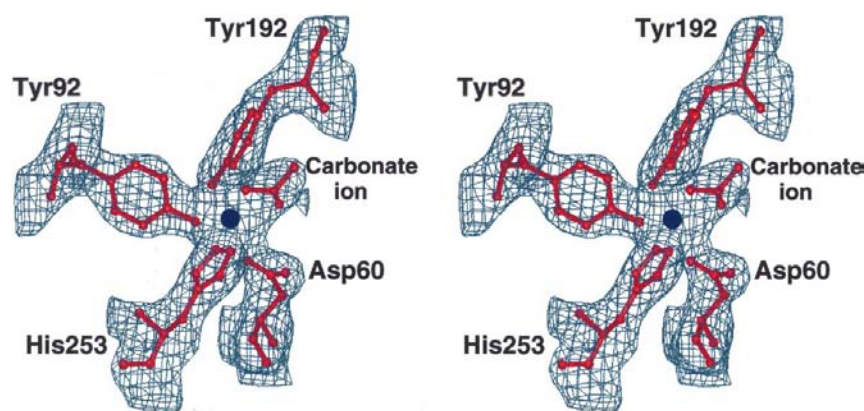

Figure 4
Stereoview of the $2F_o - F_c$ electron-density map at the iron-binding site for the N lobe. The electron density at the C lobe iron-binding site is very similar. The map is contoured at 1.2σ.

Table 4
Distances (Å) of the metal- and anion-binding sites.

The numbers in parentheses indicate corresponding residues in the C lobe. The number of digits given do not necessarily reflect the accuracy of the values.

	N lobe	C lobe
Metal–ligand		
Fe—OD1 Asp60 (395)	2.25	1.98
Fe—OH Tyr92 (433)	1.94	2.08
Fe—OH Tyr192 (526)	1.93	2.01
Fe—NE2 His253 (597)	2.09	2.06
Fe—O1 (carbonate)	2.11	2.09
Fe—O2 (carbonate)	2.23	2.29
Hydrogen bonds		
O2···NE Arg121 (463)	2.74	2.72
O2···NH2 Arg121 (463)	2.74	2.53
O1···N123 (465)	2.75	2.79
O3···OG Ser117 (459)	2.70	2.74
O3···N124 (466)	2.75	2.87

the non-coordinated O3 atom accepts two hydrogen bonds through its lone pairs. This results in a set of hydrogen bonds which satisfy the full hydrogen-bonding potential of the carbonate ion and allow it to fit perfectly between the Fe atom and anion-binding pocket. The geometry of the metal ligand and the hydrogen bonds involving the anion are listed in Table 4. The binding sites in the two lobes are very similar. Superposition of the two sites (Fe^{3+} and CO_3^{2-} ions, the iron ligands and the anion-binding residues, including the N-terminus residues of helix 5, a total of 74 atoms) gives an r.m.s. deviation of 0.44 Å. The deviations for the bond lengths and angles between the two sites are also small: 0.34 Å and 0.17°, respectively. The carbonate coordination is similar in both the N and C lobes, whereas in the human and mare lactoferrins it is asymmetrical in the N lobe and the C lobe, respectively. The metal binding seems to be similar in the N lobe and C lobe, on comparison of the coordination bond lengths. The metal coordination is reasonably similar to that observed in the buffalo lactoferrin structure at 277 K (Fig. 5). The superposition of the iron-binding sites of the two structures shows an r.m.s shift of 0.40 Å. The structure of buffalo lactoferrin shows the closest similarity to the structure of bovine lactoferrin (Moore *et al.*, 1997). Superpositions of the separate N- and C-terminal lobes of blf2 and clf using only the secondary-structural elements in the least-squares calculations show the structural movements in the binding sites. In the N-terminal site, the iron in blf2 is 0.3 Å from the equivalent position in clf and is displaced in a direction away from Tyr92 and towards the opening of the binding cleft. The anion has rotated in its plane by 25° about one O atom (Fig. 6).

3.7. Carbohydrate structure

The amino-acid sequence of buffalo lactoferrin suggests five potential N-glycosylation sites with Asn-*X*-Ser/Thr sequences. These are at Asn233, Asn281, Asn386, Asn476 and Asn545. In the difference Fourier maps, continuous electron density could be found only at Asn545. As the sequences of the carbohydrates are not known for the buffalo lactoferrin, further attempts to model the carbohydrate densities were not made.

3.8. Crystal packing

The solvent calculation on buffalo lactoferrin shows that the crystals contain 57.6% solvent, which is slightly higher than the crystals grown at 277 K (55%). For the whole molecule of 689 amino-acid residues, there are 30 strong interactions in the present structure, whereas there were only nine in the structure
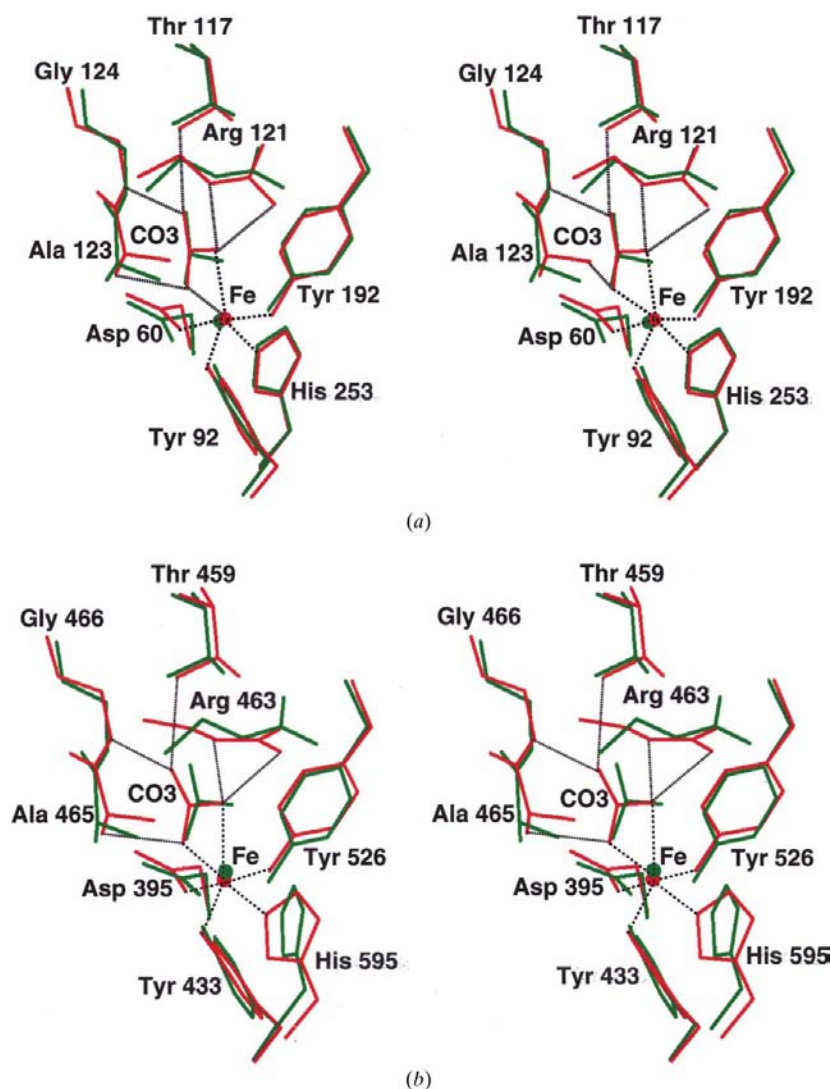

Figure 5
Stereoview of the (*a*) N-lobe and (*b*) C-lobe metal-binding sites of diferric buffalo lactoferrin at 303 K (red) superimposed on buffalo lactoferrin at 277 K (green). The hydrogen bonds associated with anion– and metal–ligand bonds are indicated for the diferric buffalo lactoferrin structure (303 K).

at 277 K. Even though the solvent content is higher at 303 K, the packing of the molecules is more favourable for the generation of a large number of intermolecular contacts.

3.9. The dilysine trigger residues

The two lysine residues (serum transferrin, Lys206 and Lys296; ovotransferrin, Lys209 and Lys301; human lactoferrin, Arg201 and Lys301; buffalo, bovine and mare lactoferrins, Lys210 and Lys301) are of special significance in the proteins of the transferrin family, as their presence seems to influence iron binding and release (Baker & Lindley, 1992; Dewan *et al.*, 1993). The amino groups of these two lysines in transferrin and ovotransferrins form hydrogen bonds with each other (Kurokawa *et al.*, 1995). In buffalo, bovine and mare lactoferrins, these lysines do not interact (Fig. 7). The equivalent residues Arg210 and Lys301 in human lactoferrin are also in similar conformations as the lysines observed in bovine, buffalo and mare lactoferrins. Examination of the amino-acid sequences of transferrins suggest that the Lys–Lys arrange-

ment is a common occurrence in them. The pH-sensitive dilysine trigger should effect lobe opening at a pH value somewhat higher than that observed in lactoferrins.

The conformation of Lys301 is similar in all the lactoferrins, but it is different from the conformations of the corresponding residues in transferrins and ovotransferrins. In buffalo lactoferrin, Lys301 NZ forms a salt bridge with Glu216 OE2 and hydrogen bonds to the carbonyl O atom of Asp302. The amino group of Lys301 is 5.2 Å from that of Lys210. It is too distant for a hydrogen bond or a van der Waals interaction. Similar distances were observed in other lactoferrins, including human lactoferrin (Haridas *et al.*, 1995). On the other hand, in transferrins, the corresponding lysine has a different conformation, resulting in the formation of a Lys$\cdots$Lys hydrogen bond. This, the so-called 'dilysine' trigger of transferrins, appears to be a result of not just having two lysines but of a particular orientation of the second lysine. The close proximity of the two resulting positive charges and their locations might well be the driving force which opens the two domains of the protein, exposing the Fe^{3+} ion and facilitating its release. The position occupied by Lys301 NZ in buffalo lactoferrin is filled by a water molecule in the N lobe of transferrin. Similarly, the position of Lys296 NZ in transferrins is occupied by a water molecule in lactoferrins. Thus, it is clear from these results that in both lactoferrin and transferrin structures the positions of side chains of Lys210 (Lys206 in transferrins) and Lys301 (Lys296 in transferrins) are variable and may be alternatively occupied by water molecules. These observations clearly indicate that the dilysine trigger is absent in lactoferrins, suggesting that the primary function of the protein is as an Fe^{3+}-chelating antimicrobial agent with no requirement for pH-dependent Fe^{3+}-release mechanism. The differences relative to the transferrins help to explain the observation that lactoferrins retain Fe^{3+} to lower pH values than transferrins. A suggested mechanism for Fe^{3+} uptake by the transferrins (Lindley *et al.*, 1993) initially involves binding of the synergistic CO_3^{2-} anion to the open apo protein, followed by Fe^{3+} binding. It was also suggested that one of the final steps of the uptake mechanism involves ligation of Fe^{3+} by Asp, which also serves to close the two domains. As noted above, the Asp ligand has been described as a trigger for closure of the two domains upon Fe^{3+} uptake (Grossmann *et al.*, 1992).
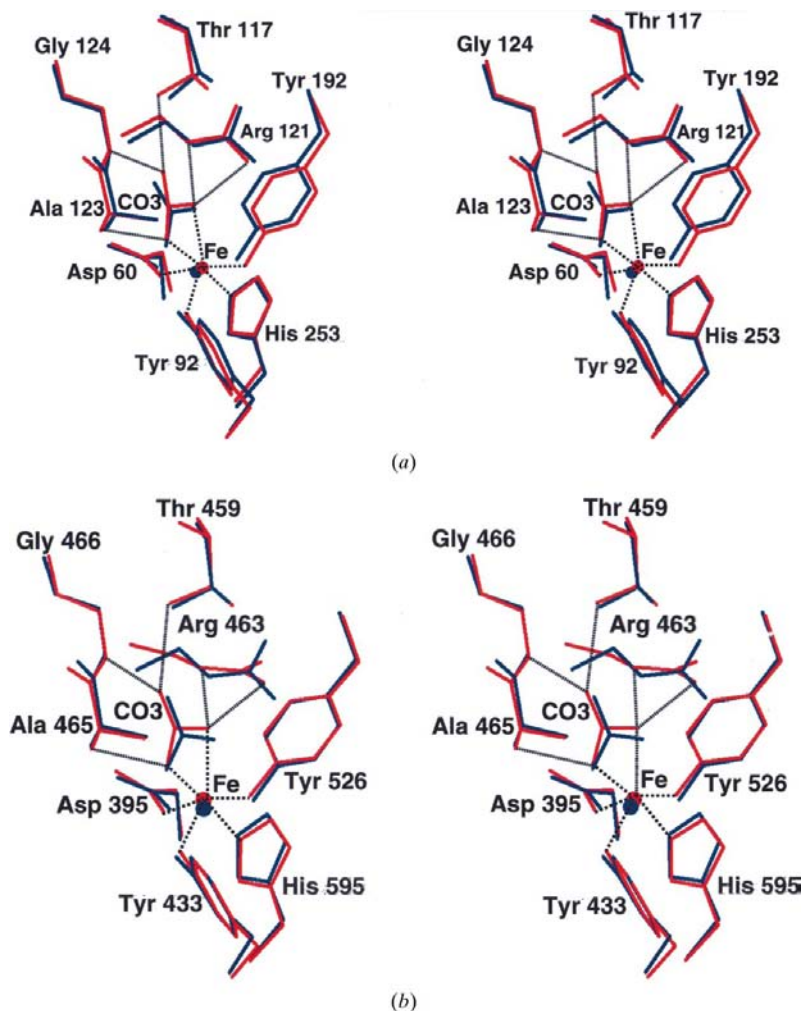

Figure 6
Stereoview of the (*a*) N-lobe and (*b*) C-lobe metal-binding sites of diferric buffalo lactoferrin at 303 K (red) superimposed on bovine lactoferrin (blue). The hydrogen bonds associated with anion– and metal–ligand bonds are indicated for the diferric buffalo lactoferrin structure (303 K).

4. Conclusions

The overall structures of buffalo lactoferrin at 277 and 303 K are similar. Superposition of these structures reveals that the relative orientations of the two lobes are considerably different. The inter-lobe interactions are predominantly hydrophobic in nature. External factors, such as the
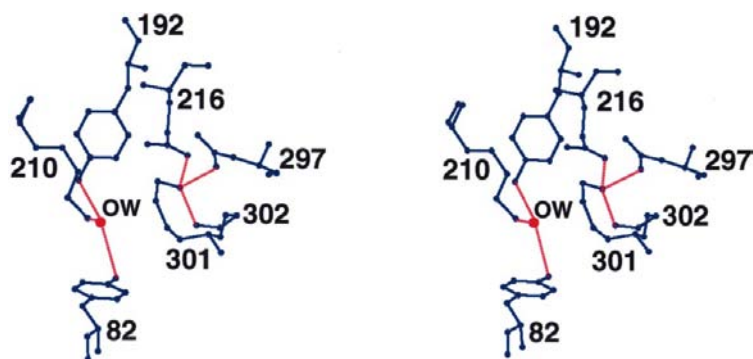
Figure 7
Stereoview of the environment behind the metal-binding site in the N lobe, showing the interactions of Lys210 and Lys301. Lys210 froms a hydrogen bond to Tyr192 and Tyr82 through a water molecule which is conserved in lactoferrins. Lys301 interacts with Glu216, Asp297 and the carbonyl O atom of Asp302. In transferrins, the corresponding Lys209 and Lys301 interact to form a so-called Lys–Lys trigger.

changes in solvent composition, temperature fluctuations and crystal packing, seem to influence the orientations of the two lobes. The two molecular halves of lactoferrin generated proteolytically using proteinase K tended to aggregate in the gel-filtration column. This fact is consistent with the structural data. On the other hand, the domain orientations do not seem to alter because of external conditions. It has previously been inferred that the domain arrangements changes drastically under the influence of crystal packing (Rawas *et al.*, 1997). In the structure of the iron-free form of duck ovotransferrin, both lobes have open conformations. Surprisingly, in the iron-free form of human lactoferrin, the N lobe adopted an open conformation, while the C lobe was found to be in the closed conformation. Also surprising was the case of the iron-free form of mare lactoferrin, where both lobes were found to be in the closed conformation. It was believed that in the iron-free forms of lactoferrins, both conformations existed in equilibrium and the crystal packing determined the state of domain association. It is very difficult to correlate this with crystal packing, as both lobes are closed in mare lactoferrin. Further studies may be needed. However, in case of iron-bound lactoferrins, the domain orientations are unaffected by crystal packing and other environmental fluctuations, but the lobe orientations change considerably. Therefore, it can be clearly stated that the conformational flexibility in iron-bound lactoferrins appears to be related to the movements of lobes and not the domains.

References

Anderson, B. F., Baker, H. M., Norris, G. E., Rice, D. W. & Baker, E. N. (1989). *J. Mol. Biol.* **209**, 711–734.

Anderson, B. F., Baker, H. M., Norris, G. E., Rumball, S. V. & Baker, E. N. (1990). *Nature (London)*, **344**, 784–787.

Arnold, R. R., Cole, M. F. & McGhee, J. R. (1977), *Science*, **197**, 263–265.

Bailey, S., Evans, R. W., Garratt, R. C., Gorinsky, B., Hasnain, S., Horsburgh, C., Jhoti, H., Lindley, P. F., Mydin, A., Sarra, R. & Watson, J. (1988). *Biochemistry*, **27**, 5804–5812.

Baker, E. N. & Lindley, P. F. (1992). *J. Inorg. Biochem.* **47**, 147–160.

Birgens, H. S., Hansen, N. E. & Kristensen, L. (1983). *Br. J. Haematol.* **54**, 383–391.

Brünger, A. T. (1992a). *X-PLOR v3.1 User's Guide. A System for X-ray Crystallography and NMR.* New Haven, Connecticut: Yale University Press.

Brünger, A. T. (1992b). *Nature (London)*, **355**, 472–474.

Brünger, A. T., Krukowski, A. & Erickson, J. (1990). *Acta Cryst.* A**46**, 585–593.

Brünger, A. T., Kuriyan, J. & Karplus, M. (1987). *Science*, **235**, 458–460.

Collaborative Computational Project, Number 4 (1994). *Acta Cryst.* D**50**, 760–763.

Dewan, J. C., Mikami, B., Hirose, M. & Sacchettini, J. C. (1993). *Biochemistry*, **32**, 11963–11968.

Grossmann, J. G., Neu, M., Pantos, E., Schwab, F. J., Evans, R. W., Townes-Andrews, E., Lindley, P. F., Appel, H., Thies, W. G. & Hasnain, S. S. (1992). *J. Mol. Biol.* **225**, 811–819.

Haridas, M., Anderson, B. F. & Baker, E. N. (1995). *Acta Cryst.* D**51**, 629–646.

Hashizume, S., Kuroda, K. & Murakami, H. (1983). *Biochim. Biophys. Acta*, **763**, 377–382.

He, J. & Furmanski, P. (1995). *Nature (London)*, **373**, 721–724.

Jones, T. A., Zou, J.-Y., Cowan, S. W. & Kjeldgaard, M. (1991). *Acta Cryst.* A**47**, 110–119.

Kabsch, W. (1986). *J. Appl. Cryst.* **21**, 916–924.

Karthikeyan, S., Sharma, S., Sharma, A. K., Paramasivam, M., Yadav, S., Srinivasan, A. & Singh, T. P. (1999). *Curr. Sci.* **77**, 241–255.

Karthikeyan, S., Yadav, S., Paramasivam, M., Srinivasan, A. & Singh, T. P. (1999). *Acta Cryst.* D**55**. Submitted.

Kraulis, P. J. (1991). *J. Appl. Cryst.* **21**, 916–924.

Kurokawa, H., Mikami, B. & Hirose, M. (1995). *J. Mol. Biol.* **254**, 196–207.

Laemmli, U. K. (1970). *Nature (London)*, **227**, 680–682.

Laskowski, R. A., MacArthur, M. W., Moss, D. S. & Thornton, J. M. (1993). *J. Appl. Cryst.* **26**, 283–291.

Lindley, P. F., Garratt, R. C., Hasnain, S. S., Jhoti, H., Kuser, P., Neu, M., Patel, K., Sarra, R., Strange, R. & Walton, A. (1993). *Acta Cryst.* D**49**, 292–304.

Matthews, B. W. (1968). *J. Mol. Biol.* **33**, 491–497.

Matthews, B. W. (1972). *Macromolecules*, **5**, 818–819.

Mazurier, J. & Spik, G. (1980). *Biochim. Biophys. Acta*, **629**, 399–408.

Moore, S. A., Anderson, B. F., Groom, C. R., Haridas, M. & Baker, E. N. (1997). *J. Mol. Biol.* **274**, 222–236.

Navaza, J. (1994). *Acta Cryst.* A**50**, 157–163.

Otwinowski, Z. & Minor, W. (1997). *Methods Enzymol.* **276**, 307–326.

Ramachandran, G. N. & Sasisekaran, V. (1968). *Adv. Protein Chem.* **23**, 283–438.

Raman, A., Bhatia, K. L., Singh, T. P., Srinivasan, A., Betzel, Ch. & Mallick, R. C. (1992). *Arch. Biochem. Biophys.* **294**, 319–321.

Rawas, A., Muirhead, H. & Williams, J. (1996). *Acta Cryst.* D**52**, 631–640.

Rawas, A., Muirhead, H. & Williams, J. (1997). *Acta Cryst.* D**53**, 464–468.

Sharma, A. K., Paramasivam, M., Srinivasan, A., Yadav, M. P. & Singh, T. P. (1999). *J. Mol. Biol.* **289**, 303–317.

Sharma, A. K., Rajashankar, K. R., Yadav, M. P. & Singh, T. P. (1999). *Acta Cryst.* D**55**, 1152–1157.

Singh, T. P., Sharma, S., Karthikeyan, S., Betzel, Ch. & Bhatia, K. L. (1998). *Proteins Struct. Funct. Genet.* **33**, 30–38.

Wootton, I. D. P. (1964). *Microanalysis in Medical Biochemistry.* 4th ed, p. 124. London: Churchill.